Plant Molecular Biology
https://doi.org/10.1007/s11103-019-00833-x

The *Arabidopsis thaliana* transcription factor MYB59 regulates calcium signalling during plant growth and stress response

Elisa Fasani[1] · Giovanni DalCorso[1] · Alex Costa[2] · Sara Zenoni[1] · Antonella Furini[1]

Received: 26 June 2018 / Accepted: 26 January 2019

Abstract

Key message **Transcription factor MYB59 is involved in plant growth and stress responses by acting as negative regulator of Ca signalling and homeostasis.**

Abstract The *Arabidopsis thaliana* transcription factor MYB59 is induced by cadmium (Cd) and plays a key role in the regulation of cell cycle progression and root elongation, but its mechanism of action is poorly understood. We investigated the expression of *MYB59* and differences between wild-type plants, the *myb59* mutant and *MYB59*-overexpressing lines (obtained by transformation in the mutant genotype) during plant growth and in response to various forms of stress. We also compared the transcriptomes of wild-type and *myb59* mutant plants to determine putative MYB59 targets. The *myb59* mutant has longer roots, smaller leaves and smaller cells than wild-type plants and responds differently to stress in germination assay. Transcriptomic analysis revealed the upregulation in the *myb59* mutant of multiple genes involved in calcium (Ca) homeostasis and signalling, including those encoding calmodulin-like proteins and Ca transporters. Notably, *MYB59* was strongly induced by Ca deficiency, and the *myb59* mutant was characterized by higher levels of cytosolic Ca in root cells and showed a modest alteration of Ca transient frequency in guard cells, associated with the absence of Ca-induced stomatal closure. These results indicate that MYB59 negatively regulates Ca homeostasis and signalling during Ca deficiency, thus controlling plant growth and stress responses.

Keywords *Arabidopsis thaliana* · Ca signalling and homeostasis · Plant growth · MYB transcription factor · Stomata · Stress response

Introduction

The MYB superfamily of transcription factors is present in all eukaryotic organisms (Lipsick 1996; Rosinski and Atchley 1998), and is characterized by the presence of 1–5 imperfect direct repeats of the R sequence responsible for DNA binding (Ogata et al. 1995; Du et al. 2009). In contrast to the relatively small number of MYB proteins in animals and fungi (Weston 1998), the MYB superfamily has expanded massively in plants and is probably the largest group of transcription factors (Riechmann et al. 2000). Plant MYB proteins can be assigned to four classes based on the number of R repeats (Dubos et al. 2010) with the most common class in plants being MYB-R2R3 (138 of the 197 MYB transcription factors in *Arabidopsis thaliana*; Katiyar et al. 2012).

Since the discovery of maize C1 MYB protein (Paz-Ares et al. 1987), hundreds of plant *MYB* genes have been functionally characterized revealing diverse roles in processes such as primary and secondary metabolism, development, lateral organ polarity, biotic and abiotic stress responses, circadian clock regulation and hormone signalling (Yanhui et al. 2006; Dubos et al. 2010). Numerous R2R3-MYB proteins play a role in the regulation of different branches of the phenylpropanoid biosynthetic pathway (Nesi et al. 2001; Mehrtens et al. 2005; Zhou et al. 2009), as well as in stress response (Cominelli et al.

Elisa Fasani and Giovanni DalCorso equally contributed to this work.

Electronic supplementary material The online version of this article (https://doi.org/10.1007/s11103-019-00833-x) contains supplementary material, which is available to authorized users.

✉ Antonella Furini
antonella.furini@univr.it

[1] Department of Biotechnology, University of Verona, Strada Le Grazie 15, 37134 Verona, Italy

[2] Department of Life Sciences, University of Milano, 20133 Milan, Italy

Published online: 01 February 2019

2005; Liang et al. 2005; Liu et al. 2014; Chezem et al. 2017; Liao et al. 2017).

The function of *A. thaliana* MYB59 (At5g59780) is still poorly defined. *MYB59*, together with its close paralogue *MYB48* (At3g46130), has been included in the R2R3 subfamily (Stracke et al. 2001), although the primary RNAs of both genes undergo alternative splicing to yield four mRNA isoforms differing only in the nature of the DNA-binding domain. Interestingly, both R2R3 and 1R/MYB-like proteins are encoded by the *MYB59* locus: the type-1 and type-2 transcripts contain only the R3 domain, the type-3 transcript encodes a classical R2R3-MYB transcription factor, and the type-4 transcript is produced by non-canonical splicing, is present at minimal levels and possibly does not encode a protein at all (Li et al. 2006a). *MYB59* is expressed at higher levels in the roots of *A. thaliana* plants (Mu et al. 2009) and particularly in the xylem during secondary cell wall growth (Oh et al. 2003). In leaves, it is induced by exposure to salicylic acid or cadmium (Cd), the latter similarly to its ortholog *BjCdR12* in *Brassica juncea* (Yanhui et al. 2006; Fusco et al. 2005). *MYB59* expression is also positively modulated in the early phases of jasmonate treatment, where it participates in association with MYB48 in the regulation of defence against pathogens (Hickman et al. 2017). In addition, *MYB59* is induced during the light-to-dark transition (Li et al. 2006b) and is regulated by the circadian cycle with peak expression in the evening, probably due to its regulation by CIRCADIAN CLOCK ASSOCIATED 1 (CCA1) which is expressed in the morning (Lai et al. 2012). MYB59 may participate in the regulation of the cell cycle, mitosis and root growth by controlling the duration of metaphase via the induction of the cyclin gene *CYCB1;1* (Mu et al. 2009). Recently, potassium (K) deficiency was found to induce differential alternative splicing of both *MYB59* and *MYB48*, suggesting a role for this transcription factor in the inhibition of root growth during K starvation (Nishida et al. 2017).

We investigated the function of MYB59 in more detail, specifically its participation in abiotic stress responses and plant growth, by comparing the transcriptomes of wild-type and *myb59* mutant plants. Our initial results indicated that MYB59 is involved in calcium (Ca) signalling, so we analysed the role of MYB59 in the context of cytosolic Ca levels and Ca-dependent stress responses. Taken together, our data indicate a new role for MYB59 in the control of Ca homeostasis and signalling, leading ultimately to the regulation of plant growth and stress responses.

Results

Expression analysis of *MYB59* splicing isoforms

Arabidopsis thaliana MYB59 was previously shown to be expressed mainly in the roots (Mu et al. 2009) and to be upregulated in response to Cd, like its ortholog *BjCdR12* in *B. juncea* (Fusco et al. 2005; Yanhui et al. 2006). Therefore, the expression of the three main splicing isoforms of *MYB59* was tested in the shoots and roots of plants growing under hydroponic control conditions. The results confirmed that *MYB59* was transcribed at higher levels in the roots than the shoots (Mu et al. 2009; Fig. 1a). Furthermore, the three main isoforms were expressed at comparable levels in leaves, whereas *MYB59.1* and *MYB59.3* were dominant in the roots (Online Resource 1a). We also evaluated *MYB59* expression following brief and prolonged exposure to 10 µM $CdSO_4$, compared to control conditions without Cd. A moderate induction in leaves was observed after 6 h, whereas a significant increase in the expression of all three isoforms in the roots occurred after Cd exposure for four days (Fig. 1b, Online Resource 1b). *MYB59* expression was also tested following exposure to drought, 250 mM NaCl or 5 µM abscissic acid (ABA) for 6 h. All three isoforms were strongly repressed in the roots in response to all treatments, whereas salinity stress and ABA caused a moderate induction of *MYB59* expression in the shoots, and drought stress produced moderate downregulation (Fig. 1c, Online Resource 1c).

The *myb59* mutant has smaller leaves due to smaller cells and altered cell cycle progression

MYB59 was previously reported to regulate cell growth and the cell cycle in the roots (Mu et al. 2009). Therefore, to determine the role of *MYB59* in plant growth, we compared wild-type plants with the *myb59* knockout mutant and transgenic plants overexpressing *MYB59* in the *myb59* mutant genotype (OE), after confirming the expression of all three main *MYB59* isoforms (Online Resource 2). We found that the mutant plants have longer roots but smaller leaves than wild-type control plants, whereas both OE lines were phenotypically comparable to wild-type plants (Fig. 2). The analysis of protoplasts from leaves 4 and 11 of 4-week-old plants indicated that the *myb59* mutant has significantly smaller leaf cells than wild-type plants, whereas the overexpression of *MYB59* in the *myb59* genotype restores the normal cell size (Fig. 3; Online Resource 3). There were no differences in the auxin content of whole leaves (IAA concentration of 1.15 ± 0.10 ng/g fresh weight (FW) in wild-type leaves and 1.09 ± 0.05 ng/g FW in *myb59* leaves).

The analysis of PI-marked nuclei by flow cytometry highlighted the altered cell cycle progression in *myb59* mutant plants compared to wild-type controls. Specifically, although the proportion of apoptotic, S and G2 nuclei was approximately the same in the leaves of both genotypes (ca. 3%, 17% and 31%, respectively), the proportion of the other stages varied greatly. The percentage of G0/G1 nuclei decreased from 35% in the wild-type leaves to 19.4% in the

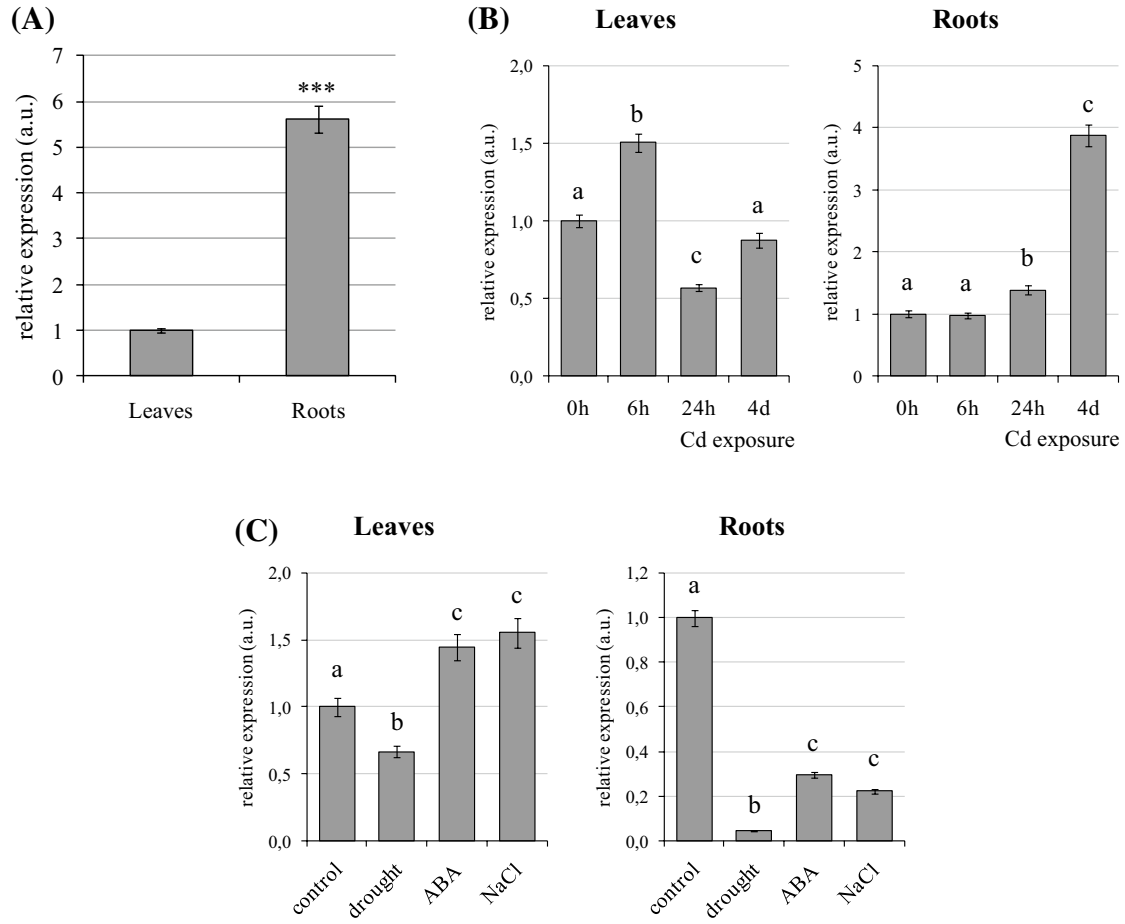

Fig. 1 Semi-quantitative analysis of *MYB59* expression by real-time RT-PCR in response to abiotic stress. **a** Expression in leaves and roots of 3-week-old plants of *A. thaliana*. **b** Expression after 6 and 24 h and 4 days of treatment with 10 µM $CdSO_4$. **c** Expression after 6 h under drought, 250 mM NaCl or 5 µM ABA treatments. Asterisks above the histogram in **a** indicate statistical significance, evaluated by Student's *t* test: $p < 0.001$. Different letters above the histograms in **b, c** indicate statistical significance, evaluated by Welch's ANOVA followed by a Games–Howell post-hoc test ($p < 0.05$)

mutant leaves, whereas polyploid nuclei were more abundant in the *myb59* mutant (29%) than in wild-type leaves (14.1%) (Fig. 4).

The *myb59* mutant tolerates Cd and salinity stress better than wild-type plants

The *MYB59* expression analyses previously presented in this work indicate that metal, salinity and ABA stress modulate *MYB59* transcription (Fig. 1c); therefore, we tested the *myb59* mutant, wild-type and OE lines for their ability to tolerate Cd, NaCl and ABA. Cd tolerance was evaluated under both standard (3 mM $CaCl_2$) and low (0.5 mM $CaCl_2$) Ca concentrations, because Cd enters the plant via Ca transporters (Hinkle et al. 1987; Perfus-Barbeoch et al. 2002) and therefore high levels of Ca can alleviate Cd stress symptoms (Huang et al. 2017). These experiments revealed that *myb59* tolerates Cd significantly better than wild-type and OE lines, as evidenced by the germination rates in low-Ca medium containing 25 µM $CdSO_4$ (Fig. 5a). We found that 10-day old *myb59* plants also had longer roots in the presence of 25 µM $CdSO_4$/3 mM $CaCl_2$ but this difference was also observed under control conditions and is probably not associated with Cd tolerance (Fig. 5b). No root growth was observed in the presence of 25 µM $CdSO_4$/0.5 mM $CaCl_2$ (data not shown). The *myb59* mutant was also moderately more tolerant to NaCl than the other genotypes, as shown by the germination assay in 50 mM NaCl (Online Resource 4a). There was no difference between genotypes in terms of root growth at both NaCl concentrations (Online Resource 4c). On the other hand, germination in the presence of ABA was impaired in the *myb59* mutant compared to wild-type and OE lines (Online Resource 4b).

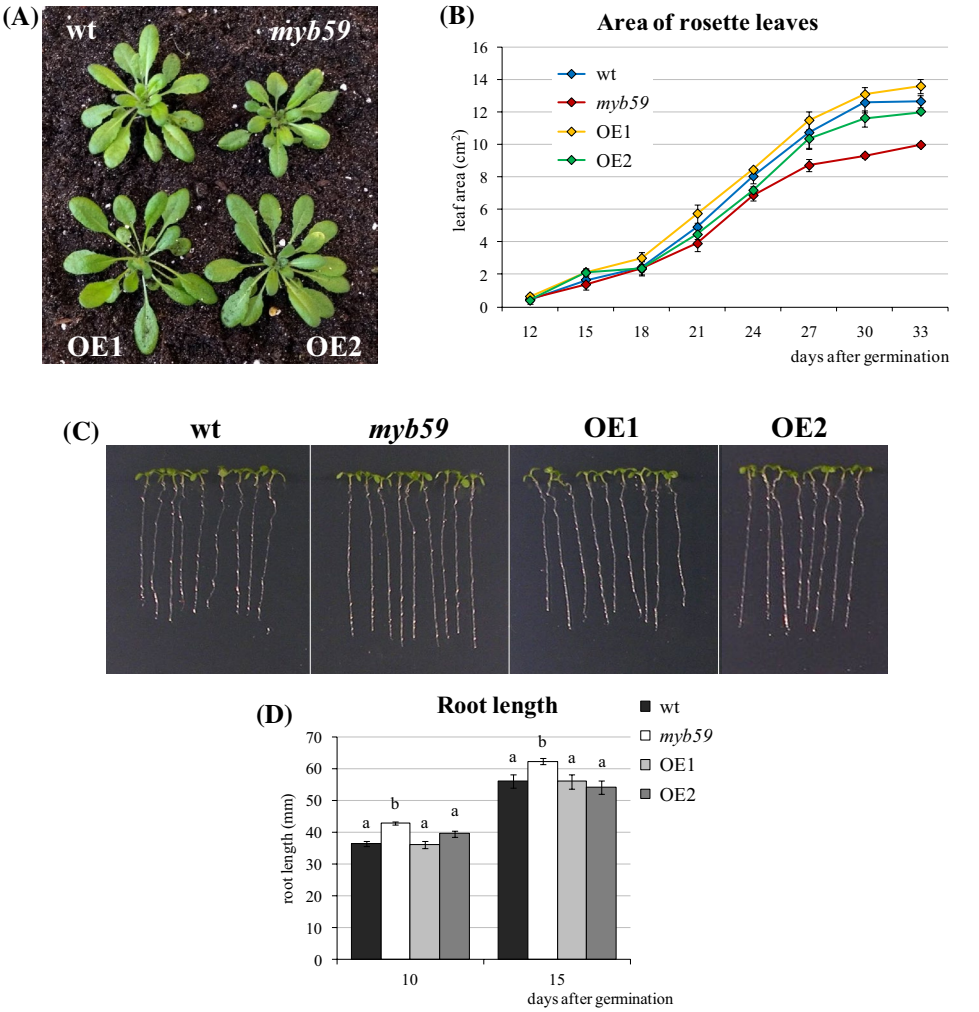

Fig. 2 Phenotype of *myb59* mutants in comparison to wild-type (wt) and overexpressing lines (OE1 and OE2). **a** Three-week-old plants grown in soil. **b** Measurement of the area of rosette leaves in time. **c** 10-day-old plantlets grown in vitro. **d** Comparison of root length 10 and 15 days after germination. Different letters above the histograms in **d** indicate statistical significance, evaluated by Welch's ANOVA followed by a Games–Howell post-hoc test ($p < 0.05$)

Transcriptomic comparison of wild-type and *myb59* plants

Microarray analysis was used for the transcriptomic comparison of wild-type and *myb59* mutant leaves from 3-week-old plants, when differential shoot growth was most apparent. The comparison revealed the presence of 45 differentially regulated transcripts, 12 of which were downregulated and 33 upregulated in the *myb59* mutant (Table 1). Among the genes upregulated in the *myb59* mutant, ca. 25% represented Ca-binding proteins and others involved in Ca homeostasis, transport and signal transduction. In particular, *ACA1* (At1g27770) and *CAX1* (At2g38170) encode Ca transporters (localized in the endoplasmic reticulum (ER) and tonoplast, respectively) and six encode EF-hand proteins potentially involved in Ca signalling: *KIC* (At2g46600) and the calmodulin-like (CML) genes *CML24* (At5g37770), *CML35* (At2g41410), *CML36* (At3g10190), *CML44* (At1g21550) and *CML47* (At3g47480). The involvement in Ca signalling was confirmed by DAVID enrichment analysis (Huang et al. 2009), revealing that the first annotation cluster (enrichment score = 4.05) included the functional classes of Ca interaction and Ca^{2+} binding. Other annotation clusters with lower enrichment scores included DNA-templated regulation of transcription, zinc finger proteins, and integral membrane components. The differential expression of several modulated genes was confirmed by real-time RT-PCR in wild-type, *myb59* and OE lines. The comparison between wild-type and *myb59* confirmed the results obtained in the microarray, with fold-changes that were generally more significant than highlighted by microarray analysis (Fig. 6). For some of the analysed genes (*NAC036, RVE2, BT2, VSP1, PDF1.1* and *CAX1*), expression in the OE lines was comparable to that of the wild-type or had an opposite modulation than that of *myb59* mutant. On the contrary, for five other genes (*CML24, CML35, CML47, KIC* and *PILS4*), mostly involved in Ca signalling, the modulation observed in OE lines was of the same sign as that of the *myb59* mutant (Fig. 6).

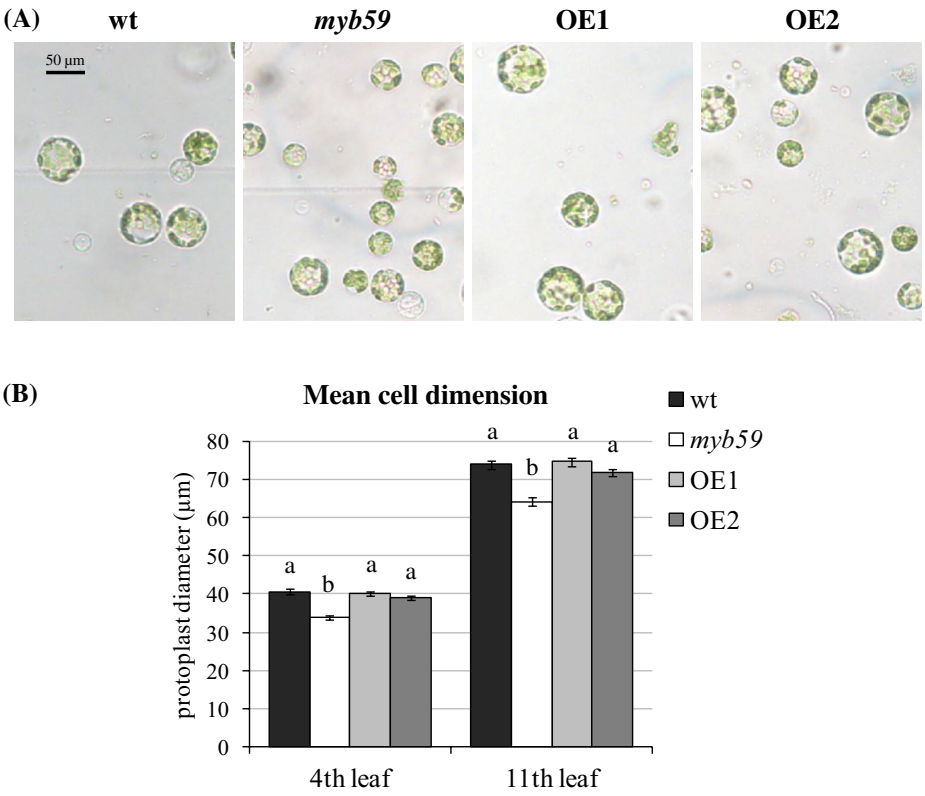

Fig. 3 Dimension analysis of protoplasts from leaf 4 and 11 of 4-week-old plants from the wild-type (wt), *myb59* mutant and overexpressing (OE1 and OE2) lines. **a** Micrographs of protoplasts from leaf 4. **b** Mean diameter of protoplasts. Different letters above the histograms indicate statistical significance, evaluated by Welch's ANOVA followed by a Games–Howell post-hoc test ($p < 0.05$)

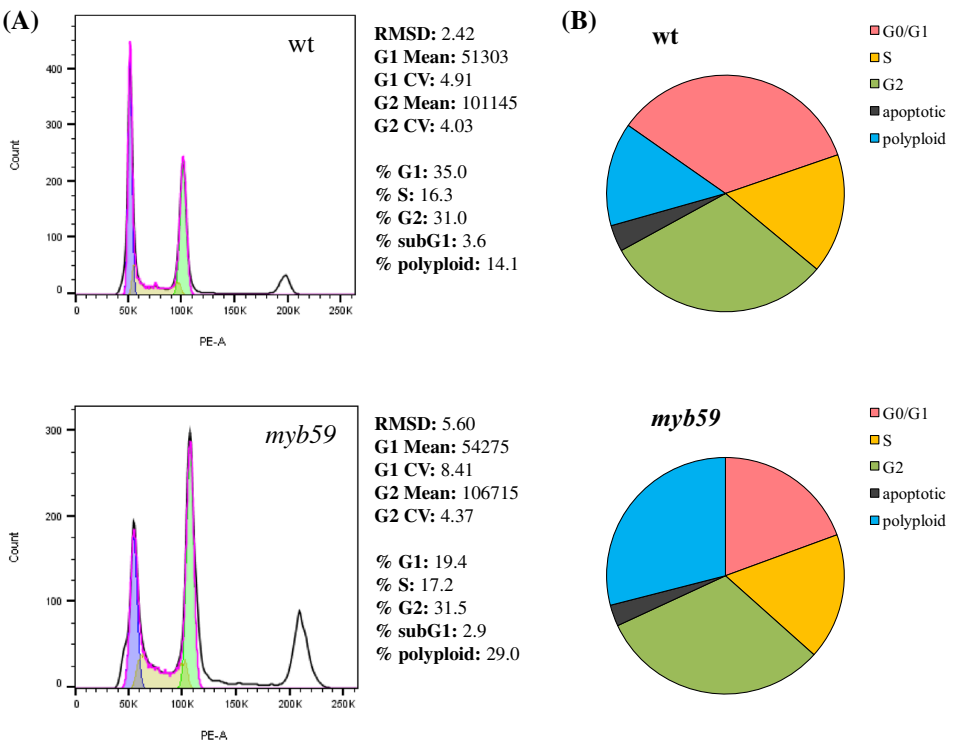

Fig. 4 Analysis of cell cycle progression by the analysis of wild-type and *myb59* nuclei in flow cytometry. **a** Distribution of nuclei with different DNA contents. **b** Frequency of nuclei in each phase of cell cycle

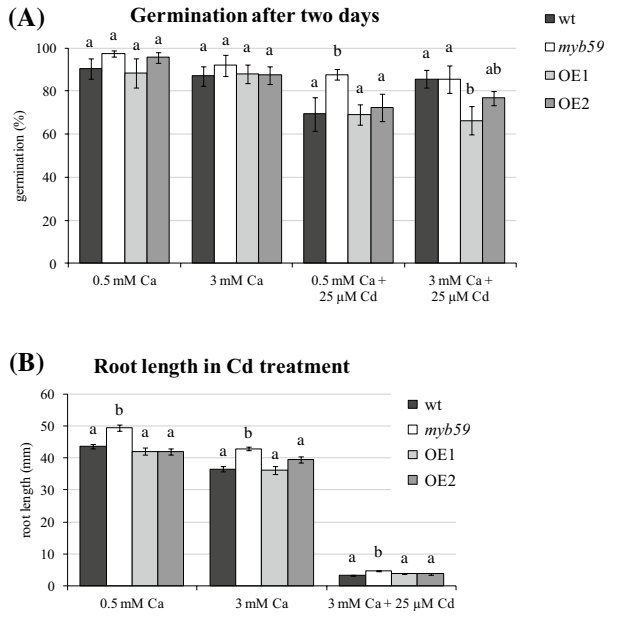

Fig. 5 Analysis of Cd tolerance. **a** Germination in absence and presence of 25 µM $CdSO_4$. **b** Root length measurement after 10 days in absence and presence of 25 µM $CdSO_4$. Different letters above the histograms indicate statistical significance, evaluated by Welch's ANOVA followed by a Games–Howell post-hoc test ($p < 0.05$)

MYB59 expression in response to Ca deficiency

Microarray analysis suggested that MYB59 is probably involved in Ca homeostasis and signalling. We therefore investigated *MYB59* expression in response to low Ca levels by growing wild-type plants in hydroponic trays in the presence of either 0.5 mM (low) or 2.5 mM (normal) $Ca(NO_3)_2$ concentrations, followed by gene expression analysis after 6, 24 and 96 h. The expression of all *MYB59* isoforms was induced in the roots by Ca deficiency at all three time points (Fig. 7, Online Resource 5). In the leaves, *MYB59* was strongly induced by Ca deficiency after 6 h but returned to normal expression levels at the subsequent time points (Fig. 7).

Genotype-specific differences in root growth do not depend on external Ca availability

To determine the response to Ca excess or deficiency, wild-type, *myb59* and OE seeds were sown *in vitro* under control conditions (3 mM $CaCl_2$), Ca excess (20 mM $CaCl_2$) or Ca deficiency (3 mM $CaCl_2$ supplemented with 1 mM or 5 mM EGTA). Since the low Ca conditions applied in previous experiments (0.5 mM $CaCl_2$) did not produce appreciable response in vitro in agarized medium (data not shown), a different experimental approach was used. The application of two different EGTA treatments allowed the generation of moderately intense and extreme Ca deficiency, respectively. Germination was approximately 100% for both genotypes under all four conditions. Root elongation after 10 days was moderately inhibited by excess Ca and severely inhibited in the presence of EGTA. The *myb59* plantlets had significantly longer roots than the other genotypes in response to all treatments, as well as under control conditions, whereas *MYB59* overexpression in the *myb59* genotype restored the wild-type phenotype (Fig. 8).

The root tips of *myb59* plants contain higher levels of cytosolic Ca

Cytosolic Ca levels were evaluated in the root tips of wild-type and *myb59* mutant plantlets transformed with the cytosolic Cameleon sensor NES-YC3.6 (Krebs et al. 2012). Wild-type and *myb59* lines expressing the NES-YC3.6 sensor were germinated and grown for 7 days under control conditions and in the presence of 25 µM $CdSO_4$, 50 mM NaCl or 1 mM EGTA. Ca levels in the cytosol of *myb59* root tip cells were slightly, yet significantly, higher than in wild-type root tips even under control conditions. In response to the three treatments, both genotypes showed an increase in cytosolic Ca levels. Interestingly, the *myb59* root tips accumulated significantly higher levels of Ca than wild-type root tips only in presence of 25 µM $CdSO_4$, whereas there was no significant difference between the two genotypes in the NaCl and EGTA treatments even though all three treatments induced an increase in the cytosolic Ca content (Fig. 9).

The *myb59* mutant is impaired in Ca-induced stomatal closure

Ca signalling plays an important role in the regulation of stomatal movement (Kim et al. 2010; Webb and Robertson 2011). Hence, based to the indications that MYB59 might be involved in the regulation of Ca signalling, we investigated whether the alteration of *MYB59* expression has an impact on stomatal physiology. After stomatal pre-opening under bright-field light, whole wild-type, *myb59* and OE leaves were either maintained in the pre-opening solution (control) or treated with 10 µM ABA, 5 mM $CaCl_2$ or 1 mM EGTA for 2.5 h. Differences were already apparent in the control experiment, where OE leaves had partially to completely closed stomata; in this situation, wild-type and *myb59* stomata showed no significant differences (Fig. 10a, b). Moreover, whereas the wild-type and OE stomata closed when exposed to Ca, the stomata in the *myb59* mutant remained significantly more open (Fig. 10a, b). Stomatal closure and complete opening were observed in the presence of ABA and EGTA, respectively, with no significant difference between the genotypes (Fig. 10a, b). The stomatal closure induced by external Ca depends on defined cytosolic

Table 1 Differentially regulated genes in leaves of the *myb59* knock-out mutant in comparison to wild-type, as resulting by microarray analysis

Gene family	MIPS code	Name	Annotation	Fold change
Down-regulated (12)				
Protein biosynthesis, modification and transport	At4g17470		Palmitoyl-protein thioesterase	−4.04
	At1g22550		Major facilitator superfamily protein	−1.80
Response to biotic stress	At5g24780	*VSP1*	Vegetative storage protein 1	−3.80
Plant growth and development	At3g15270	*SPL5*	Squamosa promoter-binding-like protein 5	−1.78
Transcription and translation	At5g61455	*U2.7*	snRNA gene U2.7	−1.51
Unknown function	At4g04223		Armadillo/beta-catenin-like repeat-containing protein	−4.07
	At3g56210		Armadillo/beta-catenin-like repeat-containing protein	−4.06
	At2g05995		Unknown gene	−1.78
	At3g29644		Potential natural antisense gene, locus overlaps with At3g29642	−1.77
	At2g18690		Unknown protein	−1.76
	At1g56050		Putative GTP-binding protein	−1.74
	At5g38005		Unknown gene	−1.54
Up-regulated (33)				
Plant growth and development	At2g46600*	*KIC*	Calcium-binding EF-hand-containing protein	3.25
	At2g17040	*NAC036*	NAC domain containing protein 36	3.23
	At2g38180		GDSL esterase/lipase	2.09
	At3g48360*	*BT2*	BTB and TAZ domain protein 2	1.94
	At5g37260	*RVE2*	Transcription factor REVEILLE 2	1.86
	At5g37770*	*CML24*	Calmodulin-like calcium-binding protein CML24	1.55
Ageing	At3g10985	*SAG20*	Senescence associated protein 20	1.71
Calcium binding	At3g47480*	*CML47*	Calmodulin-like calcium-binding protein CML47	3.67
	At2g41410*	*CML35*	Calmodulin-like calcium-binding protein CML35	2.84
	At2g38170*	*CAX1*	Vacuolar cation/proton exchanger 1	2.28
	At1g21550*	*CML44*	Calmodulin-like calcium-binding protein CML44	2.18
	At1g27770*	*ACA1*	Autoinhibited Ca^{2+}-ATPase 1	1.51
Response to biotic and abiotic stress	At5g61600	*ERF104*	Ethylene-responsive transcription factor ERF104	3.01
	At3g10190*	*CML36*	Calmodulin-like calcium-binding protein CML36	2.52
	At3g44260	*CAF1A*	Putative CCR4-associated factor 1–9	2.51
	At1g27730	*STZ, ZAT10*	Zinc finger protein STZ/ZAT10	2.18
	At1g75830	*PDF1.1*	Defensin-like protein 13	2.08
	At3g16720	*ATL2*	RING-H2 finger protein ATL2	1.99
	At1g18710	*MYB47*	MYB domain transcription factor 47	1.75
Hormone metabolism and transport	At1g76530	*PILS4*	Auxin efflux carrier-like protein	2.16
Transport	At3g53980		Bifunctional inhibitor/lipid-transfer protein/seed storage 2S albumin-like protein	2.02
Response to endogenous stimula	At5g50915	*bHLH137*	Transcription factor bHLH137	1.91
Unknown function	At1g53480	*MRD1*	*mto1* responding down 1 protein	4.86
	At2g26695		Ran BP2/NZF zinc finger-like protein	2.95
	At5g58570		Hypothetical protein	2.81
	At2g16367		Pseudogene, defensin-like (DEFL) family protein	2.79
	At3g19030		hypothetical protein	2.35
	At3g43060		Pseudogene, hypothetical protein	2.31
	At5g03090		Hypothetical protein, homologous to MRD1	2.15
	At5g35660		Glycine-rich protein	1.95
	At4g36850		PQ-loop repeat family protein/transmembrane family protein	1.64
	At3g28270		Hypothetical protein	1.52

Table 1 (continued)

Gene family	MIPS code	Name	Annotation	Fold change
	At1g01390		UDP-glycosyltransferase superfamily protein	1.51

Asterisks near the MIPS code mark proteins involved in calcium homeostasis and signal transduction

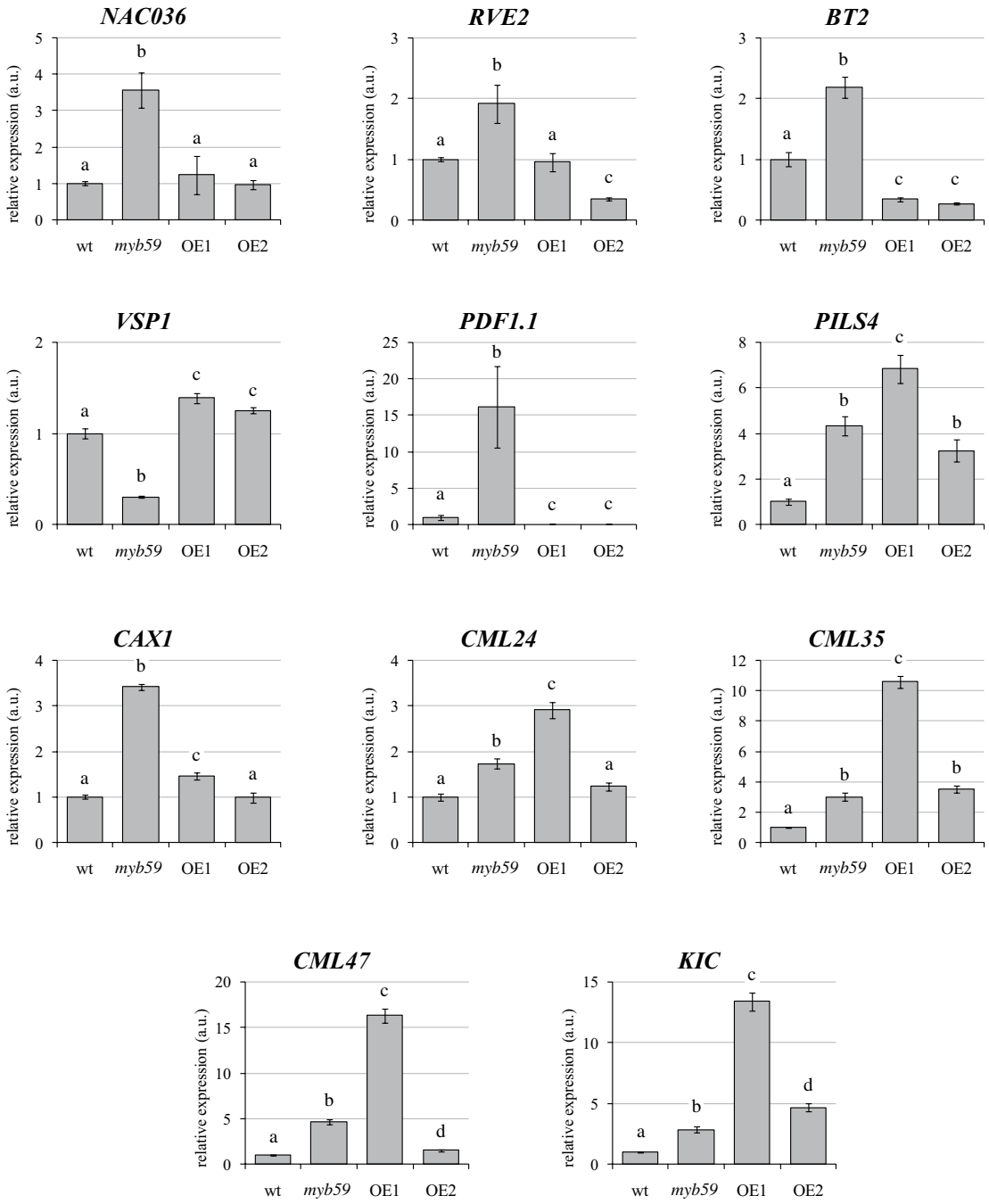

Fig. 6 Validation of microarray data. Real-time RT-PCR to confirm modulation of genes resulting by the comparative transcriptomic analysis performed between wild-type, *myb59* mutant and overexpressing (OE1 and OE2) plants grown for 3 weeks in soil in control conditions. Different letters above the histograms indicate statistical significance, evaluated by Welch's ANOVA followed by a Games–Howell post-hoc test ($p < 0.05$)

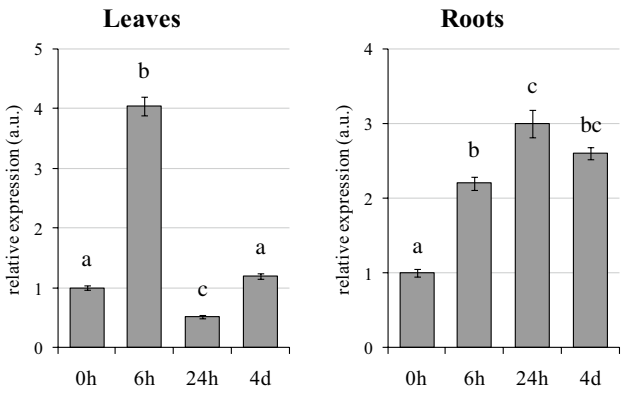

Fig. 7 Expression of *MYB59* after 6 and 24 h and 4 days under low-Ca treatment (0.5 mM $Ca(NO_3)_2$). Different letters above the histograms indicate statistical significance, evaluated by Welch's ANOVA followed by a Games–Howell post-hoc test ($p < 0.05$)

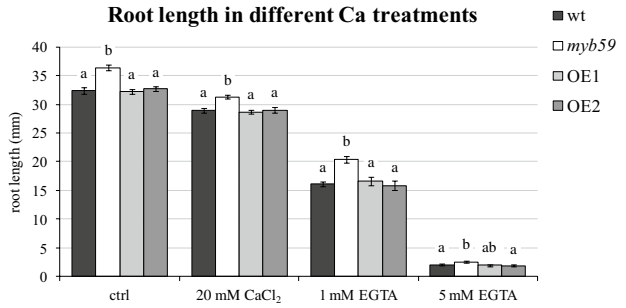

Fig. 8 Response of wild-type (wt), *myb59* mutant and overexpressing (OE1 and OE2) plants to different Ca availability: 20 mM (excess), 3 mM (control) and 3 mM $CaCl_2$ supplemented with 1 mM and 5 mM EGTA (moderate and extreme deficiency). Root length was measured after 10 days in presence of different Ca availability. Different letters above the histograms indicate statistical significance, evaluated by Welch's ANOVA followed by a Games–Howell post-hoc test ($p < 0.05$)

Ca increases in guard cells (Allen et al. 2000, 2001). To explain the different stomatal behaviour in the presence of high external Ca, the guard cells of wild-type and *myb59* plants, expressing the Cameleon NES-YC3.6 sensor, were exposed to variation of external Ca concentration in order to monitor the cytosolic Ca oscillation. The stomata of epidermal strips were pre-opened under bright-field light for 2 h and then perfused with incubation buffer for 10 min and Ca-inducing buffer (10 mM $CaCl_2$) for 20 min while measuring the fluorescence. No marked alteration was observed in the profile of cytosolic Ca, with a very low Ca peak frequency in the open stomata in incubation buffer, and a significantly higher frequency after Ca induction with the high Ca buffer (Fig. 10c). Following the administration of external Ca, the peak frequency was moderately, yet significantly, lower in the *myb59* guard cells than in wild-type controls (Fig. 10d).

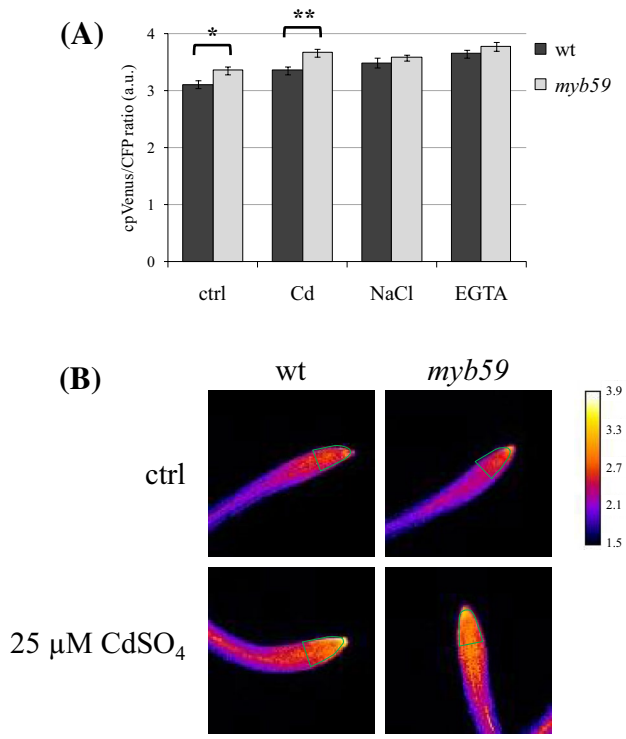

Fig. 9 Cameleon analysis of wild-type and *myb59* root tips in response to Cd, NaCl and EGTA. **a** Mean cpVenus/CFP fluorescence ratio in root tips of wild-type (wt) and *myb59* plantlets. **b** False color microscopic images of wild-type and *myb59* root tips. Green-encircled areas represent the Region of Interest (ROI) considered for the quantitative analysis. Asterisks above the histograms in **a** indicate statistical significance, evaluated by Student's *t* test: *$p < 0.05$; **$p < 0.01$

Discussion

The MYB superfamily is involved in diverse physiological processes, including cell differentiation, secondary metabolism, plant development, responses to hormones and to environmental stimuli (reviewed by Dubos et al. 2010). Regarding MYB59, a clear functional characterization has not been reached so far, since experimental evidences are relatively few and lead to a variety of apparently unrelated processes. It is proposed to participate in the development of secondary cell walls and vasculature in *A. thaliana* stems (Oh et al. 2003), in jasmonate signalling (Hickman et al. 2017) and in the response to K deficiency (Nishida et al. 2017), as well as to regulate growth and the cell cycle in roots (Mu et al. 2009). In addition, *MYB59* expression is induced by Cd and salicylic acid in *A. thaliana* (Yanhui et al. 2006) and its *B. juncea* ortholog *BjCdR12* is also upregulated following 6 h exposure to Cd (Fusco et al. 2005). However, the precise function of MYB59 remains unclear and the alternative splicing of the *MYB59* gene adds to the complexity (Li et al. 2006a).

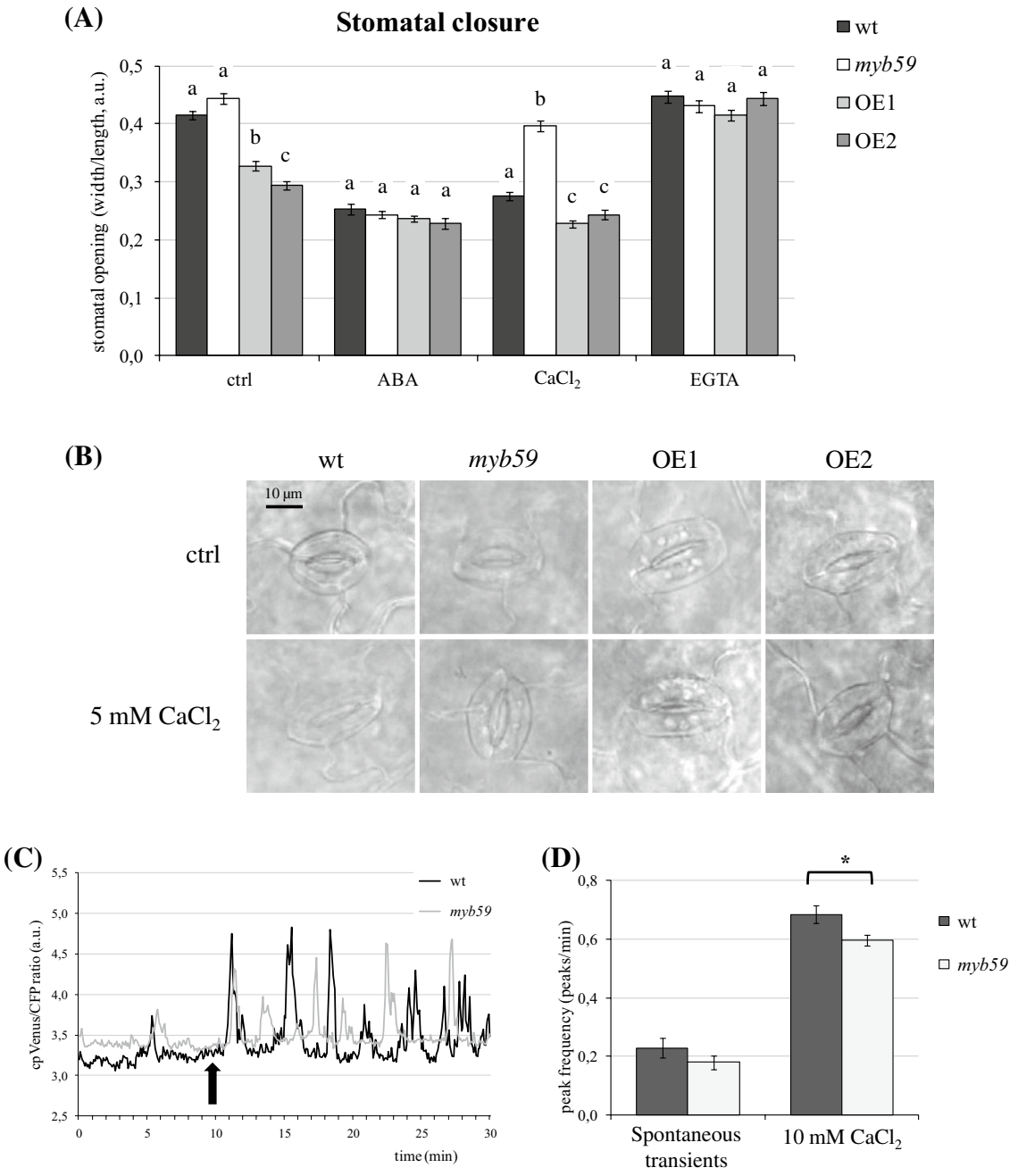

Fig. 10 Analysis of stomata aperture and Ca oscillation. **a** Measurement of stomatal opening (expressed as width/length ratio) of wild-type (wt), *myb59* and overexpressing lines (OE1 and OE2) in entire leaves treated with 10 µM ABA, 5 mM $CaCl_2$ or 1 mM EGTA. Different letters above the histograms indicate statistical significance, evaluated by Welch's ANOVA followed by a Games–Howell post-hoc test ($p < 0.05$). **b** Micrographs of stomata in control and 5 mM $CaCl_2$ conditions. **c** Cameleon analysis of wild-type and *myb59* guard cells. Stomata were pre-opened in bright-field light for 2 h in the incubation buffer. From measurement start, stomata were kept under perfusion in the incubation buffer for 10 min, then in Ca-inducing buffer (10 mM $CaCl_2$) for 20 min. Examples of Ca profile are reported for wild-type and *myb59* guard cells; the black arrow indicates the change to Ca-inducing buffer. **d** Frequency of Ca oscillation before and after the Ca-inducing buffer. Asterisks above the histograms indicate statistical significance, evaluated by Student's *t* test: *$p < 0.05$

Based on the functions suggested in previous studies (Fusco et al. 2005; Yanhui et al. 2006), we first investigated *MYB59* expression under Cd stress. For all *MYB59* transcript variants, moderate upregulation was observed in leaves after 6 h and strong upregulation was observed after four days in roots. Moreover, similar results were observed when *MYB59*

expression in leaves was tested following exposure to salinity and drought stress for 6 h, suggesting that *MYB59* responds to general stress rather than specifically to Cd. Other MYB transcription factors also mediate stress responses (Yanhui et al. 2006). For example, the ABA-responsive *A. thaliana* proteins MYB2 (Abe et al. 2003) and MYB96 (Seo et al. 2011) regulate gene expression under drought stress, with the latter also involved in salinity and freezing tolerance (Guo et al. 2013). The hypothesis of a marginal involvement of *MYB59* in stress response is also supported by the results achieved in the germination experiments in the presence of Cd and NaCl. In particular, the higher germination rate observed in the presence of Cd at low Ca for the *myb59* mutant in comparison to the wild-type and OE lines possibly correlates with the higher levels of *CAX1* observed in control conditions. Indeed, the *CAX1* gene seems to correlate with Cd tolerance in the Cd hyperaccumulator species *Arabidopsis halleri* and the loss-of-function *cax1* mutant in *A. thaliana* is more sensitive to Cd under Ca-deficiency conditions (Baliardini et al. 2015). Additionally, several other genes involved in biotic and abiotic stress responses are modulated in the *myb59* mutant already in control conditions, supporting the hypothesis that MYB59 has a role in stress response. Both positive and negative expression modulation was observed for them: for example, among the genes involved in biotic stress responses, *PDF1.1* (Plant Defensin 1.1) was strongly upregulated in *myb59*, whereas *VSP1* (Vegetative Storage Protein 1) was significantly downregulated. Consistently, recent experimental evidences suggest that MYB59 may play a dual role of activator and repressor of different defence pathways (Hickman et al. 2017). In any case, both the higher stress tolerance and the upregulation in the *myb59* mutant of genes involved in stress seem to point to a role in the negative control of stress responses, as proposed for other transcription factors (Novillo et al. 2004; Agarwal et al. 2006; Journot-Catalino et al. 2006).

In addition to the Ca transporter CAX1, the group of genes that are identified as upregulated in the *myb59* mutant compared to wild-type plants in the microarray analysis was found to be highly enriched for the functional classes Ca interaction and Ca^{2+} binding, including five CMLs (*CML24, CML35, CML36, CML44* and *CML47*), a non-CML EF-hand protein (*KIC*), another Ca transporter (*ACA1*) and the Ca-binding transcription factor *BT2* (At3g48360). The significant number of Ca-related upregulated genes strongly suggests that MYB59 plays a role in the negative regulation of Ca signalling. The role of MYB59 as a negative regulator of transcription is apparently in contrast to what observed in previous work, where MYB59 was proposed to activate transcription of the *CYCB1;1* gene in roots (Mu et al. 2009). However, as reported above, MYB59 has been suggested to work both as an activator and as a repressor of different pathways (Hickman et al. 2017).

Similarly to MYB59, MYB30 was recently found to control cytosolic Ca levels in response to stress (Liao et al. 2017). In particular, this transcription factor was proposed to confer oxidative and heat stress tolerance by moderating Ca levels via the repression of the annexin genes *ANN1* and *ANN4*, which may link the regulation of reactive oxygen species and Ca signalling pathways (Liao et al. 2017). However, the expression analysis of Ca-related genes in the OE lines highlighted a modulation of EF-hand and *PILS4* genes that is of the same sign of that measured in *myb59* mutant. This result suggests that MYB59 does not directly regulate *CML* genes. Although it is still not clear if *CML* genes are transcriptionally regulated by cellular Ca changes, this is a likely occurrence due to their role in Ca signal transduction. In this light, the altered *MYB59* expression (overexpression in OE lines and abolition in the knock-out mutant) possibly disrupts endogenous Ca homeostasis, with a subsequent alteration of *CML* expression.

In addition to the above-discussed involvement of MYB59 in stress response, the genes emerging from the microarray analysis link MYB59 also to cell growth and cell cycle progression. For example, EF-hand proteins as CML24 and KIC are involved in cytoskeletal control (Reddy et al. 2004; Tsai et al. 2013). Consistently with this, *myb59* mutant displays longer roots, as previously reported (Mu et al. 2009), together with reduced leaf area and protoplast size and altered proportion of leaf cell nuclei at different stages of the cell cycle, supporting the hypothesis that MYB59 participates in the regulation of cell cycle progression in shoots. In addition, *CAX1* and *BT2*, upregulated in the *myb59* mutant and repressed in the OE lines, are involved in the regulation of plant growth and development through Ca homeostasis/signalling. For example, *cax1* mutants have shorter primary roots than wild-type plants, which is consistent with our results (Cheng et al. 2003). By analysing both root elongation and stomatal opening, CAX1 was linked with auxin signalling (Cheng et al. 2003; Cho et al. 2012) and cell wall extensibility (Conn et al. 2011). Ca signalling, mediated by the EF-hand proteins CML12/TOUCH3 (TCH3) and PID-BINDING PROTEIN 1 (PBP1), is strictly interconnected with auxin signalling (Benjamins et al. 2003). Furthermore, this link probably includes the calmodulin-binding protein BT2 (Du and Poovaiah 2004; Ren et al. 2007; Mandadi et al. 2009). BT2 also regulates telomerase activity in vegetative organs (Ren et al. 2007) and controls seed germination in response to ABA (Mandadi et al. 2009), a process that we found to be impaired in the *myb59* mutant. The potential role of MYB59 in auxin signalling is supported by the alteration of *PILS4* expression in the *myb59* mutant and OE lines. PILS proteins are ER-localized transporters involved in subcellular auxin trafficking and compartmentalization (Barbez et al. 2012). However, we observed no difference in the IAA content of wild-type and

myb59 leaves, although this is compatible with the lack of a severe developmental phenotype in the *myb59* mutant. Nevertheless, this result does not exclude changes in the intracellular distribution of auxins, as suggested by the modulation of the *PILS4* transcript.

The role of MYB59 as negative regulator of Ca homeostasis and signalling is likely dependent on the perception of and response to specific nutritional conditions. Indeed, *MYB59* expression responds promptly to Ca deficiency, with strong upregulation in shoots 6 h after the onset of treatment and at all time points in the roots. A recent work suggests an involvement of this transcription factor in the response to K deficiency: although no definite modulation of *MYB59* transcription was observed, differential alternative splicing occurred, leading to an increase in the level of those isoforms containing both R2/R3 motifs (Nishida et al. 2017). Moreover, as indicated by the Cameleon analysis in the root tips, basal cytosolic Ca levels in *myb59* root cells are slightly higher than in wild-type plants, confirming the role in Ca homeostasis and storage. Upon Cd exposure, the cytosolic Ca levels increased in both genotypes, with the *myb59* content higher than the wild type. Considering this result and the fact that in *Saccharomyces cerevisiae* the response to Cd is dependent on specific cytosolic Ca perturbations (Ruta et al. 2014), it would be possible to hypothesize that the higher basal levels of cytosolic Ca in *myb59* mutants contribute to the partial Cd tolerance observed in this genotype.

The role of MYB59 in Ca signalling is confirmed by our analysis of stomatal behaviour, given that the *myb59* mutant lacks the ability to close its stomata in response to Ca, whereas the overexpression of *MYB59* in the mutant genotype complements the mutant phenotype. Interestingly, the Cameleon analysis of cytosolic Ca levels in guard cells indicated that the frequency of Ca pulses in high-Ca buffer is moderately lower in the *myb59* mutant compared to wild-type plants. The frequency, number and duration of Ca pulses in guard cells are known to affect stomatal opening in a specific manner (Allen et al. 2000, 2001), with lower frequencies generally correlating with more open stomata (Allen et al. 2000). For example, in the *cpk6* mutant which lacks a Ca-dependent protein kinase, the stomata are unresponsive to methyl jasmonate, and this phenotype was associated with a reduction in the frequency of cytosolic Ca pulses in guard cells and with the reduced activation of non-selective Ca^{2+}-permeable cation channels in response to the specific stimulus (Munemasa et al. 2011). In the *myb59* mutant, the abnormal expression of *CAX1* and *ACA1*, both involved in subcellular Ca storage (Huang et al. 1993; Cheng et al. 2003), and the higher basal levels of cytosolic Ca in root cells, indicate that MYB59 is involved in the regulation of Ca fluxes and therefore in stomata closure and opening. However, the difference in the frequency of stomatal Ca pulses has an high impact on stomatal closure despite being comparatively small. It is possible that MYB59 acts downstream of the Ca transient signals, as proposed for AtGLR3.1 (Cho et al. 2009) and MPK9 and MPK12 (Khokon et al. 2015), whose altered expression induced a similar situation.

It is important to notice that in control condition stomata are closed in OE lines and open in wild-type and *myb59* mutant. This evidence suggests that *MYB59* overexpression provides a constant signal for stomatal closure. Furthermore, the inhibition of stomatal closure in the presence of EGTA for all genotypes supports the hypothesis that the closure signal given by MYB59 is mediated by Ca: therefore, *MYB59* constitutive expression alters Ca transients, thus leading to an increased stomatal closure already under control conditions.

In conclusion, our results concerning the functions of MYB59 can be summarized in the model shown in Fig. 11. Our data suggest that MYB59 functions in the negative control of Ca homeostasis, signalling and subcellular compartmentalization in response to Ca deficiency and various forms of stress, contributing to the maintenance of steady cytosolic Ca levels, as well as in the modulation of Ca-mediated physiological processes, such as cell and plant growth, stomatal opening and stress responses.

Materials and methods

Plant material and growth conditions

Arabidopsis thaliana accession Columbia (Col0) and the knock-out mutant *myb59-1* (GK-627C09, from now on indicated as *myb59*) were obtained from NASC (http://arabidopsis.info; Scholl et al. 2000). The second mutant line, *myb59-2*, reported by Mu and co-workers was not considered in this work as it is a knock-down mutant displaying hardly any phenotype (Mu et al. 2009). The mutation was confirmed by PCR using the primers listed in Table 2, and

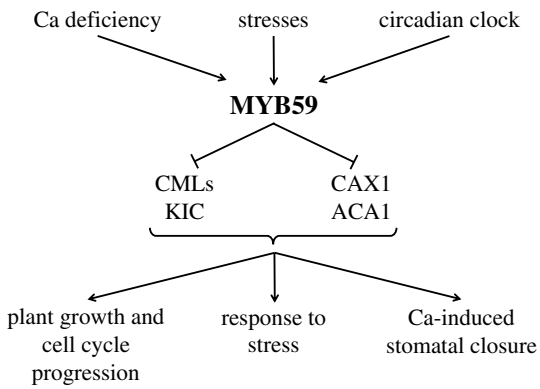

Fig. 11 Proposed model of MYB59 activity, as emerging from this work

the homozygous mutant was used for transformation (see next section) and further analysis.

For standard growth conditions, the plants were cultivated in the glasshouse in soil or in hydroponic trays at 23 °C with a 16-h photoperiod. For in vitro cultivation, seeds were sterilized with 70% ethanol for 1 min, then with 10% sodium hypochlorite containing 0.03% Triton X-100 for 15 min, and rinsed three times with sterile water. Sterile seeds were sown on solid MS medium (Murashige and Skoog 1962) supplemented, when necessary, with 3% sucrose, and vernalized for two days at 4 °C. The plants were maintained in vitro with a 16-h photoperiod at 23 °C.

Table 2 Primers used for PCR and real-time RT-PCR analysis

Function	Gene	Primer sequences 5′→3′
myb59 mutant confirmation	*MYB59* (At5g59780)	MYB59 fw: ATGAAACTTGTGCAAGAAGAATACC
		MYB59 rev: CTAAAGGCGACCACTACCATG
		LB-Gk: GCGTGGACCGCTTGCTGCAACTC
MYB59 cloning	*MYB59* (At5g59780)	Fw: TCTAGAATAAATATTGGTAAGAGGATTGCC
		Rev: CTCGAGCTAAAGGCGACCACTACCATG
Real-time RT-PCR	*β-actin* (At5g09810)	Fw: GAACTACGAGCTACCTGATG
		Rev: CTTCCATTCCGATGAGCGAT
	UBQ10 (At4g05320)	Fw: AGGACAAGGAAGGTATTCCTC
		Rev: CTCCTTCTGGATGTTGTAGTC
	MYB59 (At5g59780)	Fw: ATTTCCCTCCTCTGGCTTCT
		Rev: TAGAGGAAACTGATCAATAGCA
	MYB59.1 (At5g59780)	Fw: ATAGGTATAGGTTTGTTTTGGAA
		Rev: AACCTACAACCAAAACCAGGT
	MYB59.2 (At5g59780)	Fw: GAAACATAAGAATAGGTTTAAACA
		Rev: TGGAGTCATCTTACCACGTTT
	MYB59.3 (At5g59780)	Fw: ACTTGTGCAAGAAGAATACCG
		Rev: CTGTTCTGTTTAAACCTGAAAC
	CAX1 (At2g38170)	Fw: CATAATCATCACAGCGTTCAC
		Rev: CGACGAAGAAACAGATGGCA
	PDF1.1 (At1g75830)	Fw: TCTACCAAGAGCTCTTAATGC
		Rev: CAAAGCAACATAACATATCTGG
	CML24 (At5g37770)	Fw: GGTGATGATTCGTATTAGCAG
		Rev: AGCAGAAGATATAGAAACAACC
	CML35 (At2g41410)	Fw: TCATGTTTGATTGATGATGGTG
		Rev: TGCTTGCCGTCACAATAACC
	CML44 (At1g21550)	Fw: GATACACATGTGACATGTGTG
		Rev: AGTTTATACATCAACACATCGG
	CML47 (At3g47480)	Fw: CGATGAGTGTACAAAGATGGA
		Rev: GCTCTTCTCTATAAGCTTCAC
	KIC (At2g46600)	Fw: GCTCTTAACCAAACCGAATTC
		Rev: ATTACATAGTTCTTGGGTGAGT
	RVE2 (At5g37260)	Fw: TGTGATGATTCTGAAGATGGC
		Rev: TCCGACACTACCACTTCTGT
	PILS4 (At1g76530)	Fw: ATCGGCGTCTTGGTAGCTC
		Rev: TGGTACAAGGGTTCTGAGGT
	NAC036 (At2g17040)	Fw: TCACTGAAGCTACCGTTTGG
		Rev: GTAAGATTCTGGAGCCATGG
	BT2 (At3g48360)	Fw: TGAAGACACCAAGTGGAAGC
		Rev: AACCCCTTGTGCTTGTTCAC

Underlined nucleotides indicate restriction sites introduced for cloning

Overexpression of *MYB59* in the *myb59* mutant

The genomic sequence of *MYB59* (1042 bp, comprising the coding regions of the three *MYB59* isoforms plus the 5′ untranslated region and a 35 bp promoter region including the TATA box) was amplified and cloned in the pMD1 vector (Das et al. 2001) under the control of the 35S CaMV promoter, between the restriction sites XbaI and XhoI. The primers for *MYB59* cloning are listed in Table 2. The construct was used for the *Agrobacterium tumefaciens*-mediated transformation of the *myb59* knock-out mutant by floral dip (Clough and Bent 1998). Transformed plants were analysed by real-time RT-PCR to confirm *MYB59* expression using the primers for *MYB59* isoforms listed in Table 2. T3 plants representing two independent transgenic lines, OE1 and OE2, were used for further analysis.

Evaluation of plant growth

To study the effect of *MYB59* gene expression on vegetative growth, seeds of wild-type and *myb59* mutant and OE lines were grown in soil under standard conditions. Rosetta leaves were photographed every three days starting from the four-leaf stage until the floral stem emerged. Leaf areas were measured using the Fiji platform (Schindelin et al. 2012). About 20 plants representing each line were analysed in three biological replicates. Roots of wild-type, *myb59* and OE plants were compared by growing seedlings vertically in vitro in MS medium supplemented with 1% sucrose and measuring root length after 10 and 15 days.

Plant treatments and real-time RT-PCR

Fifteen-day-old wild-type plantlets germinated in vitro were transferred to hydroponic trays in half-strength Hoagland solution (Hoagland and Arnon 1950) and grown for a further 2 weeks. Five plants were then selected for each stress treatment, i.e. exposure to 5 µM ABA, 250 mM NaCl, or left to dry on paper for 6 h. To analyse Cd response, plants were treated with 10 µM $CdSO_4$ and sampled after 6, 24 and 96 h. To analyse the response to Ca deficiency, plants were grown in half-strength modified Hoagland's solution containing 0.5 mM $Ca(NO_3)_2$ and sampled after 6, 24 and 96 h; complete Ca deficiency was not applied since it was proved to be excessively stressful for the plant, as already observed (Nishida et al. 2017). For each analysis, untreated plants in standard half-strength Hoagland's solution (2.5 mM $Ca(NO_3)_2$) were used as a control for each time point to account for circadian regulation. Roots and shoots were sampled and analysed separately.

Total RNA from roots and shoots was extracted with TRIzol® Reagent (Thermo Fisher Scientific, Waltham, MA, USA). After DNase treatment, first-strand cDNA was synthesized using the Superscript® III Reverse Transcriptase Kit (Thermo Fisher Scientific). Real-time RT-PCR was carried out using a StepOnePlus™ Real-Time PCR System (Applied Biosystems, Foster City, CA, USA) and the KAPA SYBR® FAST ABI Prism® 2X qPCR Master Mix (Kapa Biosystems, Wilmington, MA, USA). Each reaction (40 amplification cycles) was carried out in triplicate and melting curve analysis was used to confirm the amplification of specific targets. The primers were designed to either discriminate between *MYB59* splicing isoforms or include all of them, and are listed in Table 2. Data were normalized using the two endogenous reference genes *β-actin* (At5g09810) and *ubiquitin 10* (At4g05320) and assessed using the $2^{-\Delta\Delta CT}$ method (Livak and Schmittgen 2001). The amplification efficiency of each primer pair (*c*. 2) was calculated using LinRegPCR v7.5 software (Ramakers et al. 2003). *MYB59* gene expression under control conditions was used as the standard to exclude the contribution of circadian regulation.

Analysis of cell dimensions

Protoplasts were produced from leaves 4 and 11 sourced from 4-week-old wild-type, *myb59* and OE plants grown in soil. Cell walls were digested overnight at 24 °C in the dark in MMC solution (10 mM MES, 0.5 M mannitol, 20 mM $CaCl_2$, pH 5.8) supplemented with Cellulase R-10 and Macerozyme R-10 (Duchefa Biochemie, Haarlem, The Netherlands) to a final concentration of 5 mg/ml each (Dovzhenko et al. 2003). Protoplasts were observed using a Leica DM RB microscope (Leica Microsystems GmbH, Wetzlar, Germany). The diameter of 250 protoplasts for each genotype and leaf type was measured using the Fiji platform (Schindelin et al. 2012).

Extraction of nuclei and flow cytometry

Nuclei were extracted from the extended leaves of 3-week-old wild-type and *myb59* plants grown in soil. Tissues were dissected in chopping buffer (45 mM $MgCl_2$, 30 mM sodium citrate, 20 mM MOPS, pH 7.0) and filtered through Miracloth (Merck KGaA, Darmstadt, Germany) (Galbraith 2014). Isolated nuclei were stained with 50 µg/ml propidium iodide (PI; Sigma–Aldrich, Milan, Italy) at 4 °C for 30 min and analysed by flow cytometry on a FACSCanto cytometer (Becton Dickinson, Franklin Lakes, NJ, USA). Flow cytometry and cell cycle data were analysed using FlowJo v10 (TreeStar, Ashland, OR, USA). Debris was excluded on the basis of side-scatter and FL-1 signals. Doublets were excluded by plotting the height against the area of the PI signal, and the cell cycle was analysed in PI-marked nuclei.

Measurement of indole-3-acetic acid (IAA) levels

IAA levels were measured in the leaves of 3-week-old wild-type and *myb59* plants grown in soil under control conditions. Plant material was harvested and immediately frozen in liquid nitrogen. Ground tissues were processed and IAA levels determined as previously described (Glauser et al. 2014).

Germination and root growth assays

Germination and root growth were tested in vitro under different conditions. Wild-type, *myb59* and OE seeds were sown in solid MS medium with 1% sucrose, containing alternatively ABA (20 µM and 50 µM) or NaCl (50 and 100 mM). For the analysis of germination in the presence of 25 µM $CdSO_4$, MS was supplemented with standard (3 mM $CaCl_2$) or low (0.5 mM $CaCl_2$) concentrations of Ca. For the analysis of the response to Ca, wild-type and *myb59* seeds were germinated in solid MS medium containing standard (3 mM $CaCl_2$) or high (20 mM $CaCl_2$) concentrations of Ca, and in the presence of 1 or 5 mM of the Ca-chelating agent ethylene glycol bis(β-aminoethylether)-*N,N,N′,N′*-tetraacetic acid (EGTA), to induce moderate and extreme Ca deficiency, respectively. The percentage germination was assessed after two days. Each treatment was tested in triplicate. For the analysis of root length, 20 plants were evaluated for each genotype 10 days after germination.

Microarray hybridization and analysis

Gene expression in wild-type and *myb59* plants was compared by microarray analysis. Total RNA from both lines was extracted from the leaves of 3-week-old plants grown in soil in the greenhouse. Three biological replicates were collected for each genotype. RNA was purified using TRIzol® reagent (Thermo Fisher Scientific) in association with the PureLink RNA Mini Kit (Thermo Fisher Scientific), according to the manufacturer's instructions. RNA concentration and purity were measured using a NanoDrop 1000 spectrophotometer (Thermo Fisher Scientific), and RNA integrity was assessed using the RNA 6000 Nano Kit (Agilent Technologies, Santa Clara, CA, USA) and the 2100 Bioanalyzer (Agilent Technologies).

The extracted RNA was converted to cDNA, transcribed to cRNA and labelled with cyanine 3 (Cy3) by Cy3-CTP incorporation using the LowInput QuickAmp Labeling One-Color kit (Agilent Technologies) according to the manufacturer's instructions. Cy3-labelled cRNA was purified using the RNeasy® Mini Kit (Qiagen, Redwood City, CA, USA) and quantified using a NanoDrop 1000 spectrophotometer. Samples were hybridized to a 4×44K *A. thaliana* expression microarray, design V4 (Agilent Technologies), following the manufacturer's recommended procedure. After hybridization, the chips were scanned using a G2565B microarray scanner (Agilent Technologies) and the data were extracted using Feature Extraction v11.5 (Agilent Technologies). The data were analysed using TMeV v4.8 (mev.tm4.org/): raw data were normalized based on the median centre, and differentially expressed genes were statistically validated using Student's *t*-test ($p < 0.01$). Genes with a fold change in expression higher than 1.5 were considered.

Microarray data were analysed to evaluate enrichment in specific biological functions (expressed as GO terms) using the Functional Annotation tool in DAVID (https://david.ncifcrf.gov; Huang et al. 2009). A medium classification stringency was applied, with a p-value threshold of 0.5 (the highest value provided in the analysis performed using the default setting).

To confirm the microarray data, real-time RT-PCR analysis was carried out using cDNA from the leaves of wild-type, *myb59* and OE plants as previously described. The differentially expressed genes tested and the corresponding primers are listed in Table 2.

Analysis of stomatal opening

Entire rosette leaves from 4-week-old wild-type, *myb59* and OE plants were harvested in darkness at the end of the night and then floated in a buffer containing 50 mM KCl, 10 mM MES-KOH (pH 6.15), and 100 µM $CaCl_2$ at 22 °C. Stomata were pre-opened under bright-field light (100 µE m^{-2} s^{-1}) for 2.5 h and then incubated for 2.5 h with or without the inclusion of 10 µM ABA, 5 mM $CaCl_2$ or 1 mM EGTA in the incubation medium. Following these treatments, the leaves were fixed overnight (0.1% glutaraldehyde, 4% paraformaldehyde, 0.1 M sodium phosphate buffer, pH 7.2) and decoloured in an ethanol gradient. Stomata were observed directly using a Leica DM RB microscope (Leica Microsystems GmbH). At least 60 stomata were measured for each genotype and condition. The stomatal aperture was measured using the Fiji platform (Schindelin et al. 2012) and indicated as a width/length ratio.

Plant preparation for the analysis of cytosolic calcium content

Cytosolic Ca was imaged in plants transformed to stably express Yellow Cameleon YC3.6 with cytoplasmic localization (NES-YC3.6: Krebs et al. 2012). *A. thaliana* wild-type and *myb59* plants were stably transformed by floral dip (Clough and Bent 1998) with *A. tumefaciens* strain GV3101 carrying the construct NES-YC3.6. Transformed lines were selected by visualizing YC3.6 fluorescence under a Leica MZ16 F stereomicroscope (Leica Microsystems GmbH). For each genotype, two lines displaying approximately the

same basal levels of fluorescence were considered for further analysis.

For the analysis of root tips, T2 plantlets were sown on MS medium with 1% sucrose containing 25 µM $CdSO_4$, 50 mM NaCl or 1 mM EGTA, and MS medium without supplements was used as a control. The meristematic zone of root tips from seven-day-old seedlings grown under the different experimental conditions was selected for imaging.

For the analysis of guard cells, small leaf pieces from 4-week-old T2 plants grown under standard conditions were attached to a coverslip using medical adhesive (Hollister Incorporated, Libertyville, IL, USA). The upper cell layers were gently removed with a razor blade. For the first experiment, epidermal strips were incubated in the incubation buffer (5 mM KCl, 10 mM MES, 50 µM $CaCl_2$, pH 6.15 adjusted with Tris-base) for 2 h under bright-field light (100 µE m^{-2} s^{-1}) to induce stomatal opening, then mounted in an open-top chamber and perfused first with the same buffer for 10 min and then with 10 mM of external calcium (5 mM KCl, 10 mM MES, and 10 mM $CaCl_2$, pH 6.15 adjusted with Tris-base) for 20 min.

Fluorescence microscopy

The NES-YC3.6 reporter lines were analysed using a Nikon Ti-E inverted fluorescence microscope (Nikon, Tokyo, Japan) fitted with a CFI PLAN Fluor 4x numerical aperture 0.13 dry objective for roots and a CFI PLAN APO 20x VC dry objective for guard cells. Excitation light was produced by a Prior Lumen 200 PRO fluorescent lamp (Prior Scientific Inc., Rockland, MA, USA) at 440 nm (436/20 nm) set to 50%. Images were collected using a Hamamatsu Dual CCD Camera ORCA-D2 (Hamamatsu Photonics, Hamamatsu City, Japan). The FRET CFP/YFP optical block A11400-03 (emission 1 483/32 nm for CFP and emission 2 542/27 nm for FRET) with a dichroic 510-nm mirror (Hamamatsu Photonics) was used for simultaneous CFP and cpVenus acquisitions. Exposure times were 300 ms for roots and 200 ms for guard cells, with 4 × 4 CCD binning. Images were acquired every 5 s for 1 min (root tips) and 30 min (guard cells). Filters and dichroic mirrors were purchased from Chroma Technology (Bellows Falls, VT, USA). The NIS-Element (Nikon) was used as a platform to control the microscope, illuminator, camera, and post-acquisition analysis.

Time lapses were analysed using the Fiji platform (Schindelin et al. 2012). Fluorescence intensity was determined over regions of interest (ROI) corresponding to the meristematic zone of root tips and to single guard cells. The cpVenus and CFP emissions of each ROI were used for the ratio calculation (cpVenus/CFP) and plotted versus time. Background signals were subtracted independently for both channels before calculating the ratio. At least 20 root tips and 50 guard cells were considered for each analysis.

Statistical analysis

In figures, data are represented as mean ± standard error. When two data sets (e.g. wild-type versus *myb59* mutant) were compared, the statistical significance was assessed using Student's *t* test. When more data sets were considered, the statistical significance of the data was evaluated by Welch's ANOVA, followed by a Games–Howell post hoc test, according to McDonald (2014).

Acknowledgements The authors are grateful to Dr. Gaétan Glauser of the Neuchâtel Platform of Analytical Chemistry (NPAC, Université de Neuchâtel, Switzerland) for the measurement of IAA content and to Dr. Maria Teresa Scupoli and Dr. Chiara Cavallini of the University Laboratory for Medical Research (LURM, University of Verona, Italy) for the flow cytometry analysis.

Author contributions EF performed most of the experiments and wrote the article with contribution of AF and GD, AC designed and helped with the Cameleon experiments and provided assistance in understanding the resulting data. SZ provided assistance in microarray analysis and interpretation. AF and GD conceived the project and supervised the experiments. EF and GD equally contributed to this work.

Funding Funding for E.F.'s PhD and research grant were from Italian Ministry of University and Research (MIUR).

References

Abe H, Urao T, Ito T, Seki M, Shinozaki K, Yamaguchi-Shinozaki K (2003) *Arabidopsis* AtMYC2 (bHLH) and AtMYB2 (MYB) function as transcriptional activators in abscisic acid signaling. Plant Cell 15:63–78

Agarwal M, Hao Y, Kapoor A, Dong CH, Fujii H, Zheng X, Zhu JK (2006) A R2R3 type MYB transcription factor is involved in the cold regulation of CBF genes and in acquired freezing tolerance. J Biol Chem 281(49):37636–37645

Allen GJ, Chu SP, Schumacher K, Shimazaki CT, Vafeados D, Kemper A, Hawke SD, Tallman G, Tsien RY, Harper JF, Chory J (2000) Alteration of stimulus-specific guard cell calcium oscillations and stomatal closing in *Arabidopsis det3* mutant. Science 289:2338–2342

Allen GJ, Chu SP, Harrington CL, Schumacher K, Hoffmann T, Tang YY, Grill E, Schroeder JI (2001) A defined range of guard cell calcium oscillation parameters encodes stomatal movements. Nature 411(6841):1053–1057

Baliardini C, Meyer CL, Salis P, Saumitou-Laprade P, Verbruggen N (2015) *CATION EXCHANGER1* cosegregates with Cadmium tolerance in the metal hyperaccumulator *Arabidopsis halleri* and plays a role in limiting oxidative stress in *Arabidopsis* spp. Plant Physiol 169:549–559

Barbez E, Kubeš M, Rolčík J, Béziat C, Pěnčík A, Wang B, Rosquete MR, Zhu J, Dobrev PI, Lee Y, Zažímalovà E (2012) A novel putative auxin carrier family regulates intracellular auxin homeostasis in plants. Nature 485(7396):119–122

Benjamins R, Ampudia CS, Hooykaas PJ, Offringa R (2003) PINOID-mediated signaling involves calcium-binding proteins. Plant Physiol 132(3):1623–1630

Cheng NH, Pittman JK, Barkla BJ, Shigaki T, Hirschi KD (2003) The *Arabidopsis cax1* mutant exhibits impaired ion homeostasis,

development, and hormonal responses and reveals interplay among vacuolar transporters. Plant Cell 15(2):347–364

Chezem WR, Memon A, Li FS, Weng JK, Clay NK (2017) SG2-type R2R3-MYB transcription factor MYB15 controls defense-induced lignification and basal immunity in *Arabidopsis*. Plant Cell 29(8):1907–1926

Cho D, Kim SA, Murata Y, Lee S, Jae SK, Nam HG, Kwak JM (2009) De-regulated expression of the plant glutamate receptor homolog *AtGLR3.1* impairs long-term Ca^{2+}-programmed stomatal closure. Plant J 58(3):437–449

Cho D, Villiers F, Kroniewicz L, Lee S, Seo YJ, Hirschi KD, Leonhardt N, Kwak JM (2012) Vacuolar CAX1 and CAX3 influence auxin transport in guard cells via regulation of apoplastic pH. Plant Physiol 160(3):1293–1302

Clough SJ, Bent AF (1998) Floral dip: a simplified method for Agrobacterium-mediated transformation of *Arabidopsis thaliana*. Plant J 16:735–743

Cominelli E, Galbiati M, Vavasseur A, Conti L, Sala T, Vuylsteke M, Leonhardt N, Dellaporta SL, Tonelli C (2005) A guard-cell-specific MYB transcription factor regulates stomatal movements and plant drought tolerance. Curr Biol 15(13):1196–1200

Conn SJ, Gilliham M, Athman A, Schreiber AW, Baumann U, Moller I, Cheng NH, Stancombe MA, Hirschi KD, Webb AA, Burton R (2011) Cell-specific vacuolar calcium storage mediated by CAX1 regulates apoplastic calcium concentration, gas exchange, and plant productivity in *Arabidopsis*. Plant Cell 23(1):240–257

Das M, Harvey I, Chu LL, Sinha M, Pelletier J (2001) Full-length cDNAs: more than just reaching the ends. Physiol Genomics 6:57–80

Dovzhenko A, Dal Bosco C, Meurer J, Koop HU (2003) Efficient regeneration from cotyledon protoplasts in *Arabidopsis thaliana*. Protoplasma 222(1–2):107–111

Du L, Poovaiah BW (2004) A novel family of Ca^{2+}/calmodulin-binding proteins involved in transcriptional regulation: interaction with fsh/Ring3 class transcription activators. Plant Mol Biol 54(4):549–569

Du H, Zhang L, Liu L, Tang XF, Yang WJ, Wu YM, Huang YB, Tang YX (2009) Biochemical and molecular characterization of plant MYB transcription factor family. Biochemistry 74(1):1–11

Dubos C, Stracke R, Grotewold E, Weisshaar B, Martin C, Lepiniec L (2010) MYB transcription factors in *Arabidopsis*. Trends Plant Sci 15(10):573–581

Fusco N, Micheletto L, Dal Corso G, Borgato L, Furini A (2005) Identification of cadmium-regulated genes by cDNA-AFLP in the heavy metal accumulator *Brassica juncea* L. J Exp Bot 56(421):3017–3027

Galbraith DW (2014) Flow cytometry and sorting in *Arabidopsis*. In: Sanchez-Serrano JJ, Salinas J (eds) Arabidopsis protocols. Humana Press, Totowa, pp 509–537

Glauser G, Vallat A, Balmer D (2014) Hormone profiling. In: Sanchez-Serrano JJ, Salinas J (eds) Arabidopsis protocols. Humana Press, Totowa, pp 597–608

Guo L, Yang H, Zhang X, Yang S (2013) Lipid transfer protein 3 as a target of *MYB96* mediates freezing and drought stress in *Arabidopsis*. J Exp Bot 64:1755–1767

Hickman R, Van Verk MC, Van Dijken AJ, Mendes MP, Vroegop-Vos IA, Caarls L, Steenbergen M, Van der Nagel I, Wesselink GJ, Jironkin A, Talbot A (2017) Architecture and dynamics of the jasmonic acid gene regulatory network. Plant Cell 29:2086–2105

Hinkle PM, Kinsella PA, Osterhoudt KC (1987) Cadmium uptake and toxicity via voltage-sensitive calcium channels. J Biol Chem 262:16333–16337

Hoagland DR, Arnon DI (1950) The water-culture method for growing plants without soil. Circular 347. College of Agriculture, University of California, Berkeley

Huang LQ, Berkelman T, Franklin AE, Hoffman NE (1993) Characterization of a gene encoding a Ca^{2+}-ATPase-like protein in the plastid envelope. Proc Natl Acad Sci USA 90:10066–10070

Huang DW, Sherman BT, Lempicki RA (2009) Systematic and integrative analysis of large gene lists using DAVID bioinformatics resources. Nat Protoc 4(1):44–57

Huang D, Gong X, Liu Y, Zeng G, Lai C, Bashir H, Zhou L, Wang D, Xu P, Cheng M, Wan J (2017) Effects of calcium at toxic concentrations of cadmium in plants. Planta 245:863–873

Journot-Catalino N, Somssich IE, Roby D, Kroj T (2006) The transcription factors WRKY11 and WRKY17 act as negative regulators of basal resistance in *Arabidopsis thaliana*. Plant Cell 18(11):3289–3302

Katiyar A, Smita S, Lenka SK, Rajwanshi R, Chinnusamy V, Bansal KC (2012) Genome-wide classification and expression analysis of MYB transcription factor families in rice and *Arabidopsis*. BMC Genom 13:544

Khokon MA, Salam MA, Jammes F, Ye W, Hossain MA, Uraji M, Nakamura Y, Mori IC, Kwak JM, Murata Y (2015) Two guard cell mitogen-activated protein kinases, MPK9 and MPK12, function in methyl jasmonate-induced stomatal closure in *Arabidopsis thaliana*. Plant Biol 17:946–952

Kim TH, Böhmer M, Hu H, Nishimura N, Schroeder JI (2010) Guard cell signal transduction network: advances in understanding abscisic acid, CO_2, and Ca^{2+} signaling. Annu Rev Plant Biol 61:561–591

Krebs M, Held K, Binder A, Hashimoto K, Den Herder G, Parniske M, Kudla J, Schumacher K (2012) FRET-based genetically encoded sensors allow high-resolution live cell imaging of Ca^{2+} dynamics. Plant J 69:181–192

Lai AG, Doherty CJ, Mueller-Roeber B, Kay SA, Schippers JHM, Dijkwel PP (2012) *CIRCADIAN CLOCK-ASSOCIATED 1* regulates ROS homeostasis and oxidative stress responses. Proc Natl Acad Sci USA 109(42):17129–17134

Li J, Li X, Guo L, Lu F, Feng X, He K, Wei L, Chen Z, Qu LJ, Gu H (2006a) A subgroup of *MYB* transcription factor genes undergoes highly conserved alternative splicing in *Arabidopsis* and rice. J Exp Bot 57(6):1263–1273

Li J, Yang X, Wang Y, Li X, Gao Z, Pei M, Chen Z, Qu LJ, Gu H (2006b) Two groups of MYB transcription factors share a motif which enhances trans-activation activity. Biochem Biophys Res Commun 341:1155–1163

Liang YK, Dubos C, Dodd IC, Holroyd GH, Hetherington AM, Campbell MM (2005) AtMYB61, an R2R3-MYB transcription factor controlling stomatal aperture in *Arabidopsis thaliana*. Curr Biol 15(13):1201–1206

Liao C, Zheng Y, Guo Y (2017) MYB30 transcription factor regulates oxidative and heat stressresponses through ANNEXIN-mediated cytosolic calcium signaling in *Arabidopsis*. New Phytol 216(1):163–177

Lipsick JS (1996) One billion years of Myb. Oncogene 13:223–235

Liu L, Zhang J, Adrian J, Gissot L, Coupland G, Yu D, Turck F (2014) Elevated levels of MYB30 in the phloem accelerate flowering in Arabidopsis through the regulation of FLOWERING LOCUS T. PLoS ONE 9(2):e89799

Livak KJ, Schmittgen TD (2001) Analysis of relative gene expression data using real time quantitative PCR and the $2^{-\Delta\Delta CT}$ method. Methods 25:402–408

Mandadi KK, Misra A, Ren S, McKnight TD (2009) BT2, a BTB protein, mediates multiple responses to nutrients, stresses, and hormones in *Arabidopsis*. Plant Physiol 150(4):1930–1939

McDonald JH (2014) Handbook of biological statistics, 3rd edn. Sparky House Publishing, Baltimore

Mehrtens F, Kranz H, Bednarek P, Weisshaar B (2005) The *Arabidopsis* transcription factor MYB12 is a flavonol-specific regulator of phenylpropanoid biosynthesis. Plant Physiol 138(2):1083–1096

Mu RL, Cao YR, Liu YF, Lei G, Zou HF, Liao Y, Wang HW, Zhang WK, Ma B, Du JZ, Yuan M (2009) An R2R3-type transcription factor gene *AtMYB59* regulates root growth and cell cycle progression in *Arabidopsis*. Cell Res 19(11):1291–1304

Munemasa S, Hossain MA, Nakamura Y, Mori IC, Murata Y (2011) The Arabidopsis calcium-dependent protein kinase, CPK6, functions as a positive regulator of methyl jasmonate signaling in guard cells. Plant Physiol 155:553–561

Murashige T, Skoog F (1962) A revised medium for rapid growth and bio assays with tobacco tissue cultures. Physiol Plant 15:473–497

Nesi N, Jond C, Debeaujon I, Caboche M, Lepiniec L (2001) The *Arabidopsis TT2* gene encodes an R2R3 MYB domain protein that acts as a key determinant for proanthocyanidin accumulation in developing seed. Plant Cell 13(9):2099–2114

Nishida S, Kakei Y, Shimada Y, Fujiwara T (2017) Genome-wide analysis of specific alterations in transcript structure and accumulation caused by nutrient deficiencies in *Arabidopsis thaliana*. Plant J 91:741–753

Novillo F, Alonso JM, Ecker JR, Salinas J (2004) CBF2/DREB1C is a negative regulator of CBF1/DREB1B and CBF3/DREB1A expression and plays a central role in stress tolerance in Arabidopsis. Proc Natl Acad Sci USA 101(11):3985–3990

Ogata K, Morikawa S, Nakamura H, Hojo H, Yoshimura S, Zhang R, Aimoto S, Ametani Y, Hirata Z, Sarai A, Ishii S (1995) Comparison of the free and DNA-complexed forms of the DNA-binding domain from c-Myb. Struct Biol 2:309–320

Oh S, Park S, Han KH (2003) Transcriptional regulation of secondary growth in *Arabidopsis thaliana*. J Exp Bot 54(393):2709–2722

Paz-Ares J, Ghosal D, Wienand U, Peterson PA, Saedler H (1987) The regulatory c1 locus of *Zea mays* encodes a protein with homology to myb proto-oncogene products and with structural similarities to transcriptional activators. EMBO J 6(12):3553–3558

Perfus-Barbeoch L, Leonhardt N, Vavaddeur A, Forestier C (2002) Heavy metal toxicity: cadmium permeates through calcium channels and disturbs the plant water status. Plant J 32:539–548

Ramakers C, Ruijter JM, Lekanne Deprez RH, Moorman AFM (2003) Assumption-free analysis of quantitative real-time polymerase chain reaction (PCR) data. Neurosci Lett 339:62–66

Reddy VS, Day IS, Thomas T, Reddy AS (2004) KIC, a novel Ca^{2+} binding protein with one EF-hand motif, interacts with a microtubule motor protein and regulates trichome morphogenesis. Plant Cell 16(1):185–200

Ren S, Mandadi KK, Boedeker AL, Rathore KS, McKnight TD (2007) Regulation of telomerase in *Arabidopsis* by BT2, an apparent target of TELOMERASE ACTIVATOR1. Plant Cell 19(1):23–31

Riechmann JL, Heard J, Martin G, Reuber L, Jiang CZ, Keddie J, Adam L, Pineda O, Ratcliffe OJ, Samaha RR, Creelman R (2000) *Arabidopsis* transcription factors: genome-wide comparative analysis among Eukaryotes. Science 290:2105–2110

Rosinski JA, Atchley WR (1998) Molecular evolution of the Myb family of transcription factors: evidence for polyphyletic origin. J Mol Evol 46:74–83

Ruta LL, Popa VC, Nicolau I, Danet AF, Iordache V, Neagoe AD, Farcasanu IC (2014) Calcium signaling mediates the response to cadmium toxicity in *Saccharomyces cerevisiae* cells. FEBS Lett 588(17):3202–3212

Schindelin J, Arganda-Carreras I, Frise E, Kaynig V, Longair M, Pietzsch T, Preibisch S, Rueden C, Saalfeld S, Schmid B, Tinevez JY (2012) Fiji: an open-source platform for biological-image analysis. Nat Methods 9(7):676–682

Scholl RL, May ST, Ware DH (2000) Seed and molecular resources for Arabidopsis. Plant Physiol 124:1477–1480

Seo PJ, Lee SB, Suh MC, Park MJ, Go YS, Park CM (2011) The MYB96 transcription factor regulates cuticular wax biosynthesis under drought conditions in *Arabidopsis*. Plant Cell 23:1138–1152

Stracke R, Werber M, Weisshaar B (2001) The *R2R3-MYB* gene family in *Arabidopsis thaliana*. Curr Opin Plant Biol 4:447–456

Tsai YC, Koo Y, Delk NA, Gehl B, Braam J (2013) Calmodulin-related CML24 interacts with ATG4b and affects autophagy progression in *Arabidopsis*. Plant J 73(2):325–335

Webb AA, Robertson FC (2011) Calcium signals in the control of stomatal movements. In: Luan S (ed) Coding and decoding of calcium signals in plants. Springer, Berlin, pp 63–77

Weston K (1998) Myb proteins in life, death and differentiation. Curr Opin Genetics Dev 8:76–81

Yanhui C, Xiaoyuan Y, Kun H, Meihua L, Jigang L, Zhaofeng G, Zhiqiang L, Yunfei Z, Xiaoxiao W, Xiaoming Q, Yunping S (2006) The MYB transcription factor superfamily of *Arabidopsis*: expression analysis and phylogenetic comparison with the rice MYB family. Plant Mol Biol 60(1):107–124

Zhou J, Lee C, Zhong R, Ye ZH (2009) MYB58 and MYB63 are transcriptional activators of the lignin biosynthetic pathway during secondary cell wall formation in *Arabidopsis*. Plant Cell 21(1):248–266